

Supplementary Methods

Protein production and purification of RePC site-directed mutants. The E248A, E248D, E248R, R353A, and K1119Q mutants of *RePC* were expressed as reported for T882A with the exception that smaller, 20 L, cultures were grown. Ni²⁺-affinity chromatography was used to purify the K1119Q and E248A mutants, while a combination of Ni²⁺-affinity and anion exchange chromatography was used to purify the R353A, E248R, and E248D enzymes to homogeneity. Cells were lysed by sonication and 0.2 mg/mL lysozyme in a 1:10 ratio of cell paste to loading buffer (20 mM HEPES (pH 7.5), 200 mM NaCl, and 10 mM MgCl₂, and 5 mM β-mercaptoethanol) supplemented with 10 mM imidazole, 1 mM PMSF, 0.1 mM EGTA, 5 μM E-64, and 1 μM Pepsatin. Cell lysate was cleared by centrifugation at 64,000 × g for 0.5 h. A 10 mL column volume of Ni²⁺-NTA Profinity resin (BioRad) was manually poured and packed in a 2.5 cm diameter column and equilibrated with loading buffer. Cleared cell lysate was applied to the Ni²⁺-affinity column and the column was washed with 250 mL loading buffer containing 20 mM imidazole. The protein was eluted with a 100 mL linear gradient of 20 - 300 mM imidazole in loading buffer. E248A and K1119Q were considered pure after the Ni²⁺-column and peak fractions were pooled and dialyzed against storage buffer (10 mM HEPES (pH 7.5), 50 mM NaCl, 10 mM MgCl₂, and 1 mM TCEP). For the other mutants, protein that eluted in concentrations ≥1 mg/mL was pooled and dialyzed against loading buffer 2 (20 mM HEPES (pH 8.0), 10 mM MgCl₂, 50 mM NaCl, and 2 mM DTT). A 10 mL column volume of Q-Sepharose Fast Flow (GE Healthcare) resin was manually poured and packed in a column with a 2.5 cm diameter. The anion-exchange resin was equilibrated with loading buffer 2 and the dialyzed protein was then loaded on the column. The column was washed with 100 mL of dialysis buffer prior to elution with a 50 mM - 1 M NaCl linear gradient (100 mL total volume). Fractions were

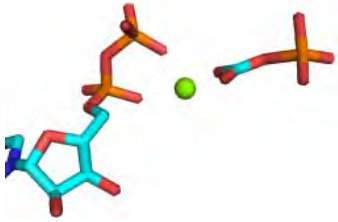
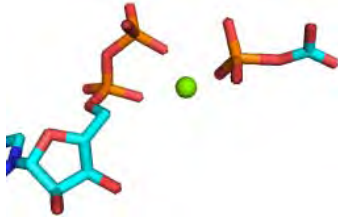
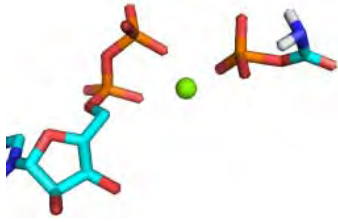
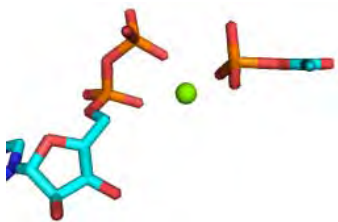
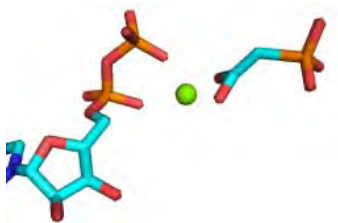
pooled and dialyzed against a storage buffer consisting of 10 mM HEPES (pH 7.5), 50 mM NaCl, 10 mM MgCl₂, and 2 mM DTT. An Amicon stirred cell was used to concentrate all proteins to 5 - 10 mg/mL. Concentrated proteins were flash frozen in liquid nitrogen prior to storage at -80 °C.

RePC Δ BC protein production and purification. The Δ BC construct of *RePC* (Δ BC-*RePC*) in a pET-28a-(His)₈-TEV plasmid was co-expressed in *E. coli* BL21Star(DE3) with *E. coli* biotin protein ligase A on vector pCY216. The Δ BC-*RePC* was expressed in M9 minimal media containing 50 μ g/mL kanamycin and 30 μ g/mL chloramphenicol. Cultures were grown at 37 °C to an Optical Density (600 nm) of 0.9 and immediately chilled on ice for 15 minutes prior to induction with 25 mM L-arabinose and 1 mM IPTG and supplementation with D-biotin to a final concentration of 1.5 mg/L. Cultures were induced at 16 °C for 18-20 hours. The Δ BC construct of *RePC* was purified using Ni²⁺-affinity chromatography as previously described (1). The purified preparation was incubated with His-tagged recombinant TEV (rTEV) protease at 4 °C (40:1 molar ratio of Δ BC *RePC* to rTEV) to remove the N-terminal (His)₈ tag of Δ BC-*RePC*. Subsequently, the sample was reapplied to a Ni²⁺-affinity column to remove the cleaved (His)₈ tag and His-tagged-rTEV protease. The (His)₈ tag cleavage and rTEV protease removal was >95% efficient as estimated by SDS-PAGE. The purified recombinant protein was concentrated to ~8 mg/mL, drop frozen in liquid nitrogen in 30 μ L aliquots and stored at -80 °C. The enzyme concentration of Δ BC-*RePC* was determined spectrophotometrically using the predicted molar extinction coefficient of 76 780 M⁻¹ cm⁻¹ at 280 nm (2).

References

1. St. Maurice, M., Reinhardt, L., Surinya, K. H., Attwood, P. V., Wallace, J. C., Cleland, W. W., and Rayment, I. (2007) Domain Architecture of Pyruvate Carboxylase, a Biotin-Dependent Multifunctional Enzyme. *Science*. 317, 1076-1079.
2. Gasteiger, E., Hoogland, C., Gattiker, A., Duvaud, S., Wilkins, M. R., Appel, R. D., and Bairoch, A. (2005) Protein Identification and Analysis Tools on the ExPASy Server, in *The Proteomics Protocols Handbook* (J. M. Walker, Ed.) pp 571-607, Humana Press.

Table S1. Table of Calculated Relative Binding Energies for Docked Analogues

Analogue	Relative Binding Energy (kcal/mol)	Conformation
Carboxyphosphate	-5.49	
	-5.12	
Carbamoyl phosphate	-4.82	
Acetyl-phosphate	-5.06	
Phosphonoacetate	-5.14	

Supplementary Figure Legends

Figure S1. Multiple cloning region sequence for the modified pET-28a vector. The open reading frame corresponding to the N-terminal (His)₈-tag and TEV cleavage site is indicated along with a number of unique restriction enzyme sites. The sites for the T7 promoter (green), lac repressor (blue), His-tag (purple) and TEV cleavage site (gold) are also indicated. This figure was generated using the program Geneious Pro (Biomatters, Ltd.).

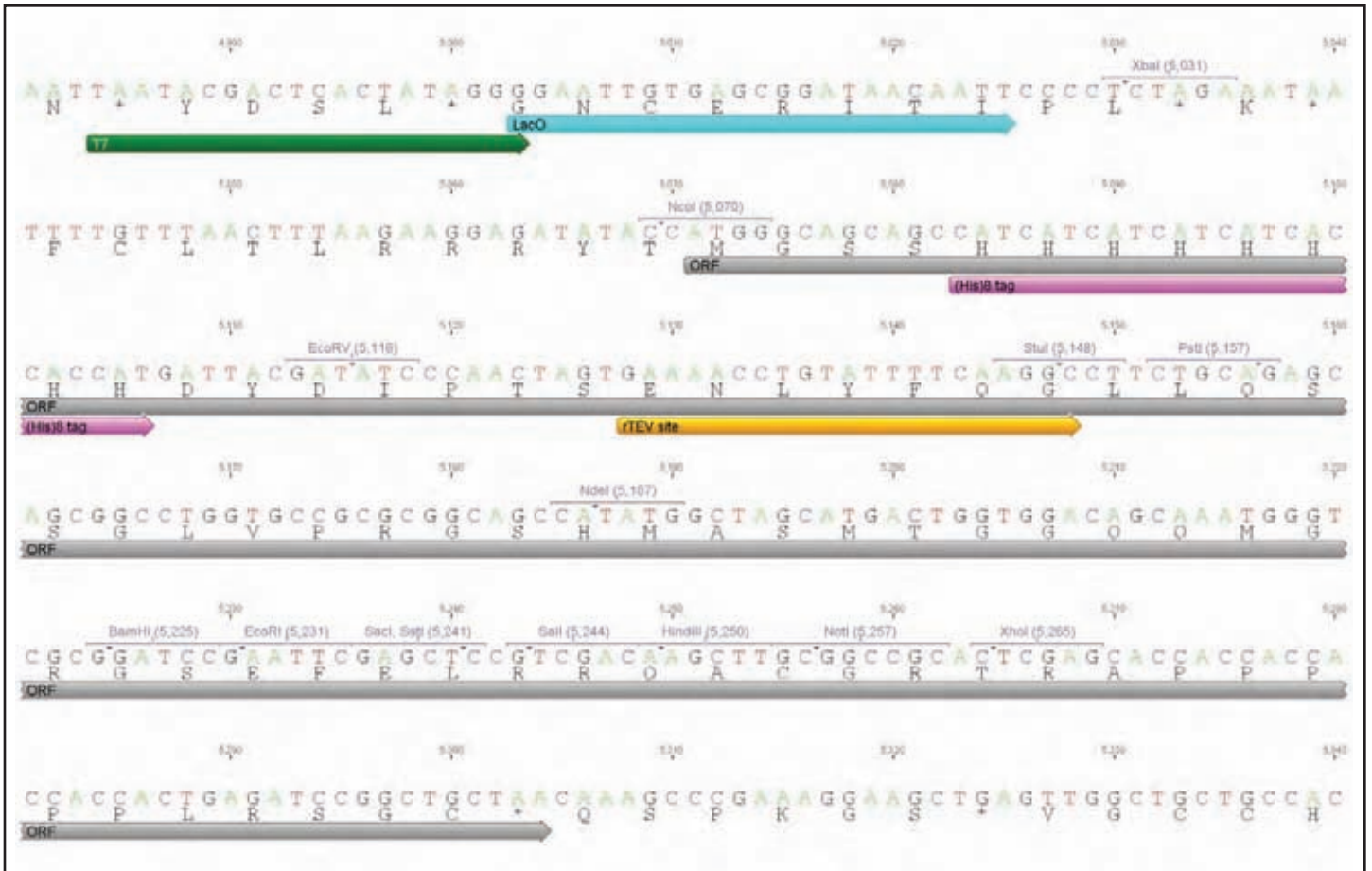
Figure S2. A bottom-side view of the two tetramers in the crystal structure of *RePC* T882A. Tetramer 1 is made up of chains A (top side; blue) and B (bottom side; yellow) while tetramer 2 consists of chains C (top side; red) and D (bottom side; green). The tetramers are presented “bottom-side up” in order to give the clearest visualization of all structural elements. Crystal packing contacts are between the two tetramers are primarily in the circled region, consisting of residues 516-538 at the periphery of the CT domain. Panels **A** and **B** are rotated 90° through the plane of the page. Panel **C** displays the structural superposition of the two tetramers, showing that they are structurally very similar, with an overall RMSD of 2.9 Å.

Figure S3. Diagrammatic scheme representing the possible rehybridization combinations of both active and inactive tetramers from mixing and diluting the T882A and K1119Q *RePC* mutants. Filled black shapes indicate an either inactive CT domain (T882A mutant) or BCCP-domain (K1119Q mutant). Red filled shapes indicate an active intermolecular catalytic pair formed across neighboring polypeptide chains.

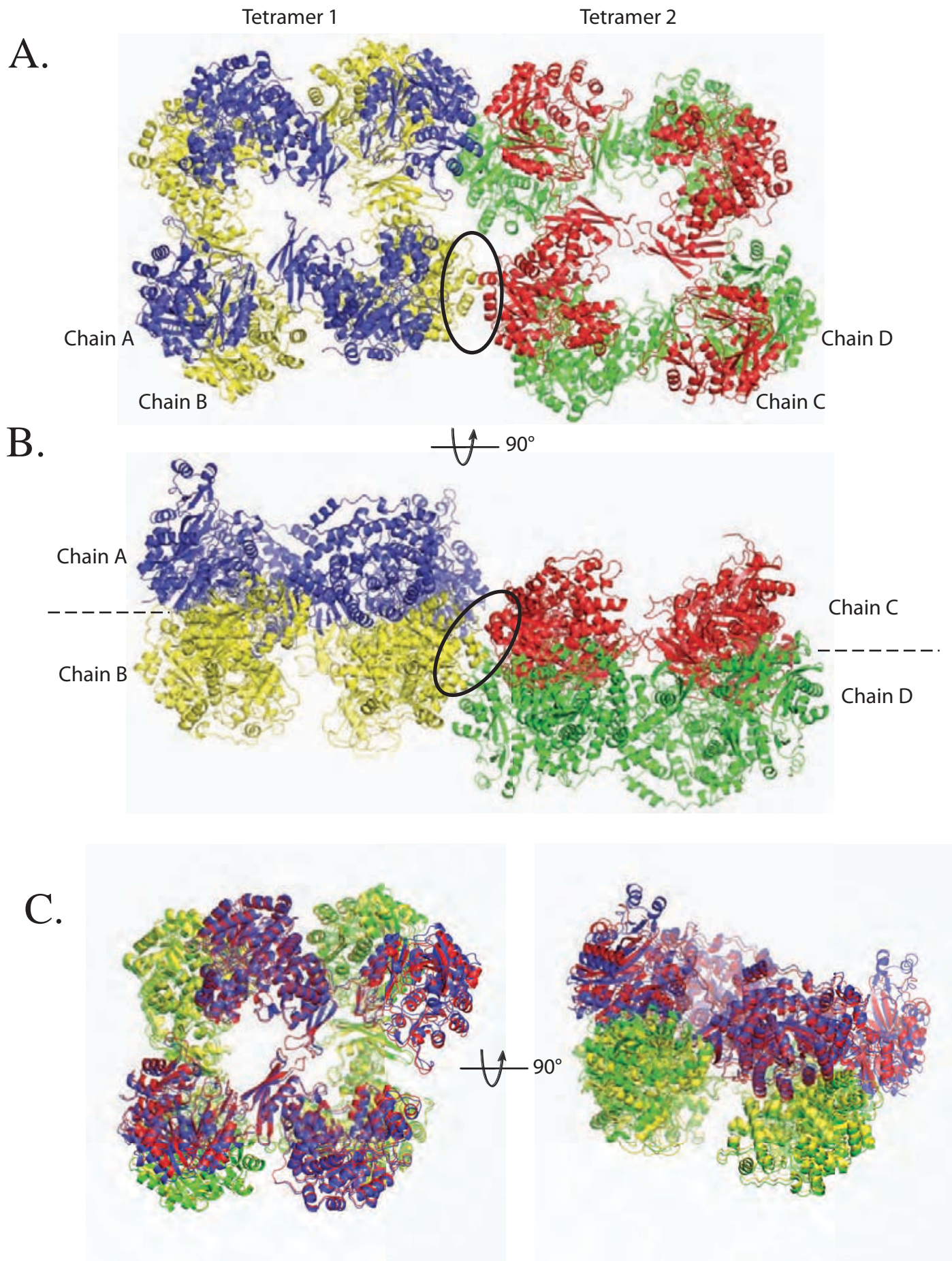
Figure S4. A side and top stereo view of the $2F_o - F_c$ electron density contoured at 1.0σ for tetramer 1 (**A**) and tetramer 2 (**B**). For clarity, the $2F_o - F_c$ electron density corresponding to the BCCP domain is colored in blue while the $2F_o - F_c$ electron density corresponding to the B-subdomain is colored in green.

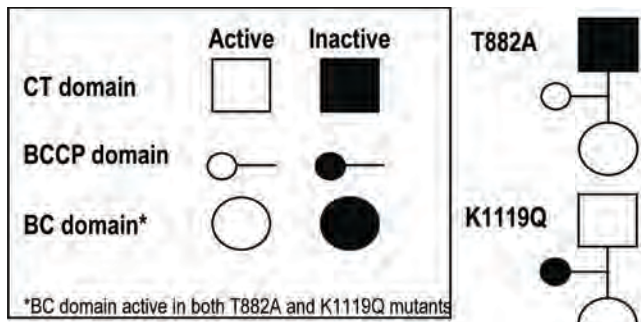
Figure S5. ClustalW sequence alignment for the BC domain of various biotin dependent carboxylase enzymes and for carbamoyl phosphate synthetase (**a**) *RePC* residues 1-250 (**b**) *RePC* residues 251-460. Yeast *pyc1* corresponds to isoform 1 of yeast PC; PCC is propionyl-CoA carboxylase; UC is urea carboxylase and CPS is carbamoylphosphate synthetase. The conservation of Arg353 and Asp248 is highlighted in a yellow starred box. Residues Tyr90 and Asp399 are also highlighted in yellow boxes.

Figure S6. Proposed reaction mechanism for the BC domain catalyzed reaction.



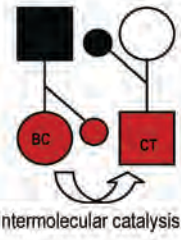
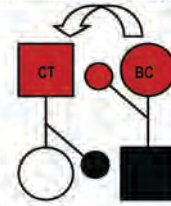
Lietzan et al.; Figure S1



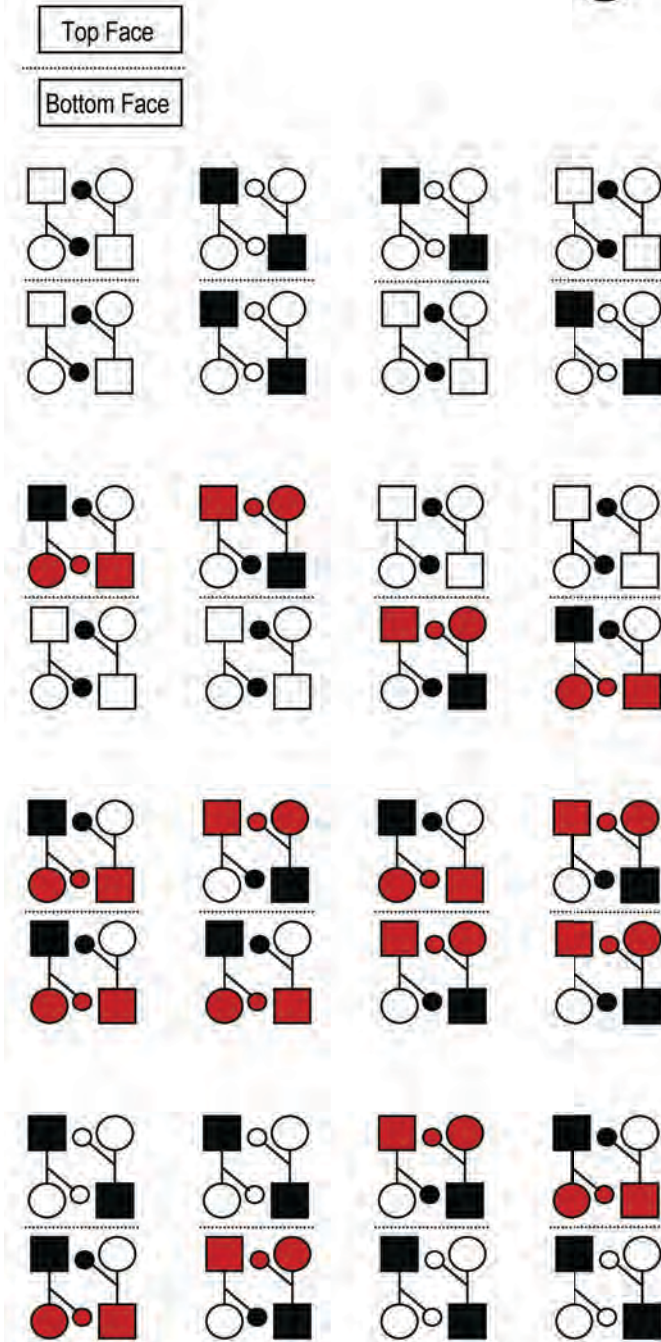


Activity arises from reassociated hybrid tetramer that allow intermolecular catalysis between **T882A BC** and BCCP domains and the CT domain of **K1119Q**

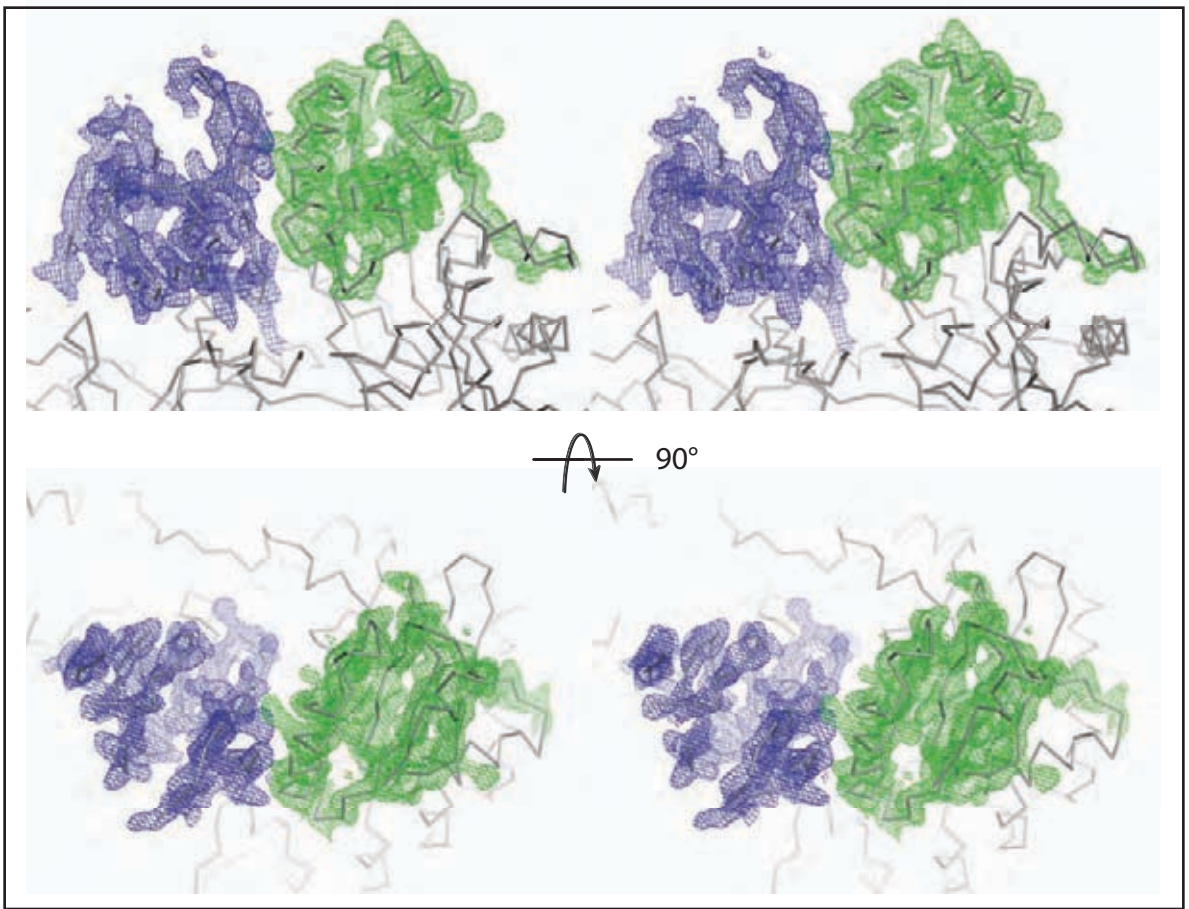
Intermolecular catalysis



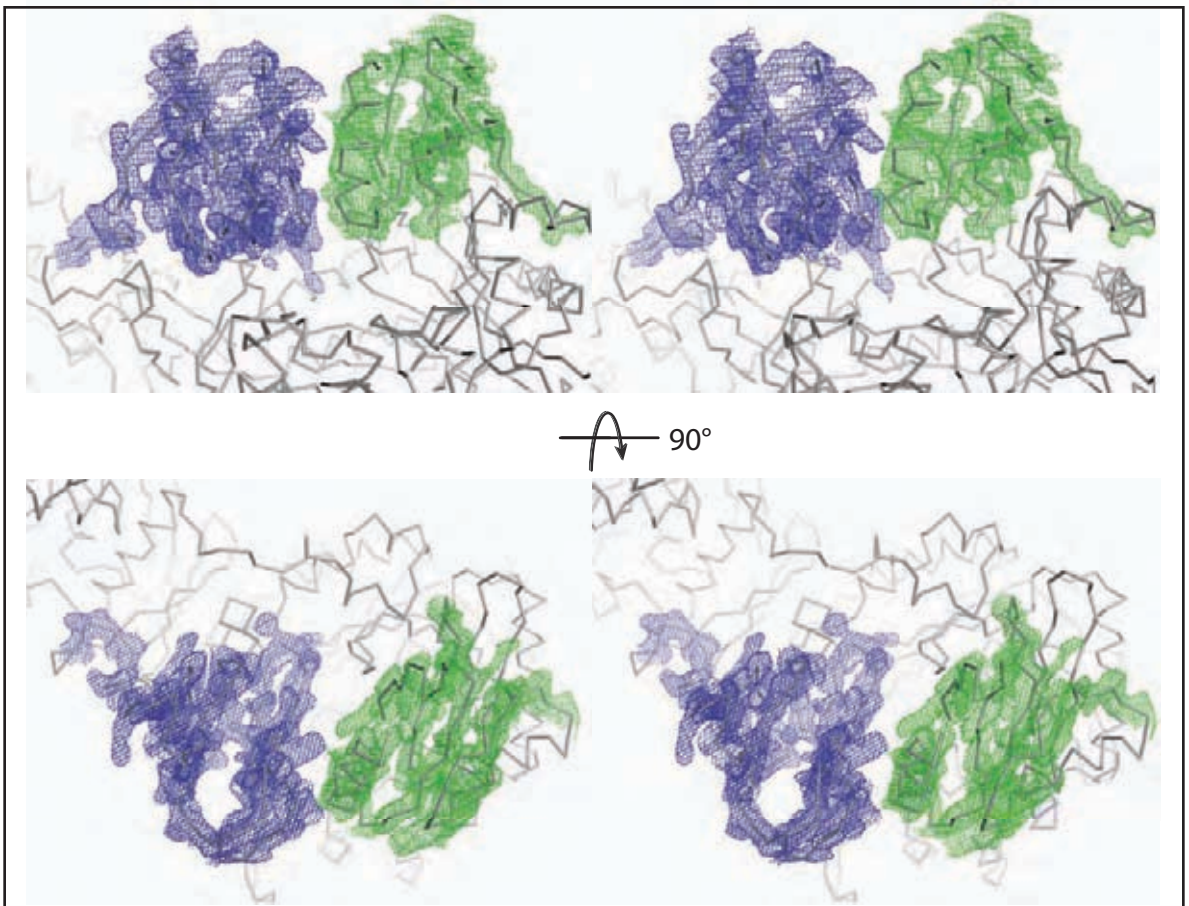
Intermolecular catalysis



A.



B.



R. coli PC	1 MPISHHVWANGHSEIAI	16	75	46	26	68	70
S. aureus PC	1 MKQINKMVAWANGHGLAI	17	25	5	58	63	71
H. sapiens PC	1 YKPIKYMVAWANGHGLAI	18	34	14	67	72	80
yeast Pyc1	1 LGKKNMVAWANGHGLPI	19	43	23	76	81	89
H. sapiens POC	1 EKTEDHVAWANGHGLAC	20	52	32	85	90	98
W. succinogenes UC	1 MFQRMVAWANGHGLAC	21	61	41	94	99	107
E. coli BC	1 MDDRMVAWANGHGLAI	22	70	50	103	108	116
E. coli CPS	1 RVDIKSLVGLGAFIVIGOACEFDYSGELICGALPREGYKVLVLSHPATIMTDPENLRTWIEE	23	79	59	112	117	125
R. coli PC	1 SGADNIEEVEYE	24	88	68	121	126	134
S. aureus PC	1 ANVDDIEEVEYE	25	97	77	130	135	143
H. sapiens PC	1 NNDVDEEVEYE	26	106	86	139	144	152
yeast Pyc1	1 HQVDIEEVEYE	27	115	95	148	153	161
H. sapiens POC	1 TRACNDEEVEYE	28	124	104	157	162	170
W. succinogenes UC	1 SGAEDHEEVEYE	29	133	113	166	171	179
E. coli BC	1 TGAVDEEVEYE	30	142	122	175	180	188
E. coli CPS	1 ERPDEIEITMGGQTAHNCALEROGVLEEHENTMIGATAKADKAEERRFDVANKKIGIET--ARSGIA-HSMEDALAVBAEVEEPE	31	151	131	184	189	197
R. coli PC	1 BSNDEGGRNEMIRSEHIDAKKEVTEKREUVAAGCKDEMTERRMERPAREHMSVQVGGCTHENVAHFERRRDSVOR	32	160	140	193	198	206
S. aureus PC	1 BTSDEGGRNEMIRREDSLEIEDAFEPKAKSPKREKSGMSERHERRRDRINPHEHREKVVQVGGCTHENVAHFERRRDSVOR	33	169	149	202	207	215
H. sapiens PC	1 BAYDEGGRNEMVHSHYEDLEENVTKAYSDEVAAGNGAERFRHREHREKVVQVGGCTHENVAHFERRRDSVOR	34	178	158	211	216	224
yeast Pyc1	1 BAPDEGGRNEMVIREGIVADALEPQATSDEKTAGNGTCTFERRREKVVQVGGCTHENVAHFERRRDSVOR	35	187	167	220	225	233
H. sapiens POC	1 BMSDEGGRNEMHAWNDRETRDGERLSQDEASSHGGDFEHEHREHREKVVQVGGCTHENVAHFERRRDSVOR	36	196	176	229	234	242
W. succinogenes UC	1 BTADEGGRNEMVGMCSMDEEERSFLTVKRLSEHREHREKVVQVGGCTHENVAHFERRRDSVOR	37	205	185	238	243	251
E. coli BC	1 BMSDEGGRNEMVIRGDIPLAQSISMTRAEKAKBSNDMTERRRREHREKVVQVGGCTHENVAHFERRRDSVOR	38	214	194	247	252	260
E. coli CPS	1 PSFETHDESSGGGLAYNREFFERFICARGLDISPTK-----EHLRRESIGRWREYERFERRRREHREKVVQVGGCTHENVAHFERRRDSVOR	39	223	203	256	261	269

Lietzan et al.; Figure S5(a)

R. etli PC 246 247 248 249 250 251 252 253 254 255 256 257 258 259 260 261 262 263 264 265 266 267 268 269 270 271 272 273 274 275 276 277 278 279 280 281 282 283 284 285 286 287 288 289 290 291 292 293 294 295 296 297 298 299 300 301 302 303 304 305 306 307 308 309 310 311 312 313 314 315 316 317 318 319 320 321 322 323 324 325 326 327 328 329 330 331 332 333 334 335 336 337 338 339 340 341 342 343 344 345 346 347 348 349 350 351 352 353 354 355 356 357 358 359 360 361 362 363 364 365 366 367 368 369 370 371 372 373 374 375 376 377 378 379 380 381 382 383 384 385 386 387 388 389 390 391 392 393 394 395 396 397 398 399 400 401 402 403 404 405 406 407 408 409 410 411 412 413 414 415 416 417 418 419 420 421 422 423 424 425 426 427 428 429 430 431 432 433 434 435 436 437 438 439 440 441 442 443 444 445 446 447 448 449 450 451 452 453 454 455 456 457 458 459 460 461 462 463 464 465 466 467 468 469 470 471 472 473 474 475 476 477 478 479 480 481 482 483 484 485 486 487 488 489 490 491 492 493 494 495 496 497 498 499 500 501 502 503 504 505 506 507 508 509 510 511 512 513 514 515 516 517 518 519 520 521 522 523 524 525 526 527 528 529 530 531 532 533 534 535 536 537 538 539 540 541 542 543 544 545 546 547 548 549 550 551 552 553 554 555 556 557 558 559 560 561 562 563 564 565 566 567 568 569 570 571 572 573 574 575 576 577 578 579 580 581 582 583 584 585 586 587 588 589 590 591 592 593 594 595 596 597 598 599 600 601 602 603 604 605 606 607 608 609 610 611 612 613 614 615 616 617 618 619 620 621 622 623 624 625 626 627 628 629 630 631 632 633 634 635 636 637 638 639 640 641 642 643 644 645 646 647 648 649 650 651 652 653 654 655 656 657 658 659 660 661 662 663 664 665 666 667 668 669 670 671 672 673 674 675 676 677 678 679 680 681 682 683 684 685 686 687 688 689 690 691 692 693 694 695 696 697 698 699 700 701 702 703 704 705 706 707 708 709 710 711 712 713 714 715 716 717 718 719 720 721 722 723 724 725 726 727 728 729 730 731 732 733 734 735 736 737 738 739 740 741 742 743 744 745 746 747 748 749 750 751 752 753 754 755 756 757 758 759 760 761 762 763 764 765 766 767 768 769 770 771 772 773 774 775 776 777 778 779 780 781 782 783 784 785 786 787 788 789 790 791 792 793 794 795 796 797 798 799 800 801 802 803 804 805 806 807 808 809 810 811 812 813 814 815 816 817 818 819 820 821 822 823 824 825 826 827 828 829 830 831 832 833 834 835 836 837 838 839 840 841 842 843 844 845 846 847 848 849 850 851 852 853 854 855 856 857 858 859 860 861 862 863 864 865 866 867 868 869 870 871 872 873 874 875 876 877 878 879 880 881 882 883 884 885 886 887 888 889 890 891 892 893 894 895 896 897 898 899 900 901 902 903 904 905 906 907 908 909 910 911 912 913 914 915 916 917 918 919 920 921 922 923 924 925 926 927 928 929 930 931 932 933 934 935 936 937 938 939 940 941 942 943 944 945 946 947 948 949 950 951 952 953 954 955 956 957 958 959 960 961 962 963 964 965 966 967 968 969 970 971 972 973 974 975 976 977 978 979 980 981 982 983 984 985 986 987 988 989 990 991 992 993 994 995 996 997 998 999 1000

Lietzan et al.; Figure S5(b)

